A Novel Active Power Filter Control Methodology

A. Yazdian-Varjani 1*, J.F. Chicharo2 and B.S.P. Perera3

- 1- Assistant Prof. of Department of Electrical Engineering Tarbiat Modarres University,
- 2- Professor of School of Electrical Engineering University of Wollongong, Australia,
- 3- Associate Prof. of School of Electrical Engineering University of Wollongong, Australia.

*P.O.Box 14115-143 Tehran, Iran yazdian@modares.ac.ir

Abstract- This paper presents a new control methodology for active power filters that provide an adaptive online harmonic estimation with partial and selective harmonic reduction schemes, which has been implemented within an integrated controller. The proposed approach is to provide partial and selective reduction of those individual harmonics which exceed the recommended levels as set by regulatory bodies reduces the rating of active power filters thus leading to cost savings. This approach contrasts with existing techniques in which the objective is to reduce all possible harmonic components to zero. Performance evaluation of the proposed technique for harmonic estimation for time-varying non-linear load is carried out when the simulation and experimental results show that the proposed control strategy provides a new alternative for harmonic reduction in power system.

Keywords: Harmonic estimation, Active power filter, Harmonic Reduction

1- Introduction

The widespread use of power electronics-based loads to improve energy efficiency and flexibility has increased the harmonic distortion levels in end use facilities and on the overall power system [1]. Regulatory organizations have increased their efforts towards establishing standards, which limit the harmonic pollution in systems [2-5]. Harmonic recommend limits on harmonic distortion in two ways. First, limits are placed on the amount of the harmonic current that consumers can inject into a utility network as a preventative action and secondly limits are imposed on the levels of harmonic voltages that are allowed to persist in the power system.

When harmonic levels exceed the compatibility limits of power system equipment, appropriate solutions should be employed for mitigation of harmonic effects on equipment. In the recent years there has been considerable

interest in the use of active filters for reducing harmonic currents in power supply systems [6-10].

Active power filters are used in power systems not only for harmonic compensation, but also for reactive power compensation and voltage control. This means that the rating of an active filter can be less than that of a passive filter for the same non-linear load. Also an active filter will not introduce system resonances that can move a harmonic problem from one frequency to another. Harmonic compensation becomes a cost-sensitive issue for customers when utilities start to enforce harmonic standards. Consequently, cost is still seen to be an obstacle for the wide spread deployment of active power filtering (APF). Therefore, the task of choosing a reliable and economical methodology for harmonic reduction from both the industrial end user and utility perspective becomes very important [11].

A reduction in active power filter rating is satisfying desirable while the minimum requirements set in the harmonic standards. This can be achieved by reducing only those harmonics that exceed the acceptable levels recommended by the respective standards. This concept could be implemented by producing an on-line estimation of the load current harmonic components. In this paper a novel control strategy suitable for a shunt active power filter has been presented which includes an on-line phase/frequency tracking, a filter bank based harmonic estimation together with a selective and partial harmonic reduction scheme. A prototype system has been developed and results indicate that the proposed approach not only works well but also provides significant benefits including a reduction of active power filter rating, incorporating of other method into harmonic reduction such as hybrid active and passive filter.

The paper is organised as follows: section 1.2 discusses in detail the proposed control strategy for the active power filter. It includes the harmonic estimation, frequency tracking and reference waveform generation. Section 1.3 describes the proposed harmonic reduction schemes including selective and partial reduction schemes. Finally, simulation test are presented and experimental results obtained from an actual prototype APF system is discussed in sections 1.4 and 1.5.

2- Active Power Filter

A functional system configuration of the proposed control strategy for active power filtering is shown in Figure 1. In this configuration, the corrective current, i_{apf} , is injected at the point of common coupling (PCC) to reduce the harmonics contained in the load current (i_{load}). The APF current, i_{apf} , can also provide fundamental reactive power compensation for the load if necessary.

2-1- Description of the Control Strategy

The flowchart of the proposed control strategy implemented on the DSP is shown in Figure 2. The process is started by sampling the load current, i_{load} , supply voltage, v_s , active power filter current, i_{apf} and DC link voltage, V_{dc} , waveforms. The phase and frequency deviation of the mains

supply ac are estimated and applied to the harmonic estimation module where selected of integer-multiple harmonics the supply frequency are estimated. The estimated harmonics are checked against the level set by the harmonic be implemented [3, 5]. If the standard to magnitudes of harmonics exceed limits, then the level recommended compensation is set to a value that reduces those harmonics just below the limit as set out by the standard or to any desired limit.

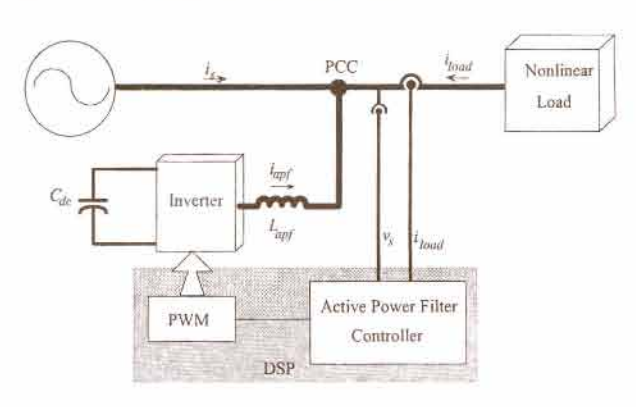


Figure 1 Functional block diagram of the proposed active power filter.

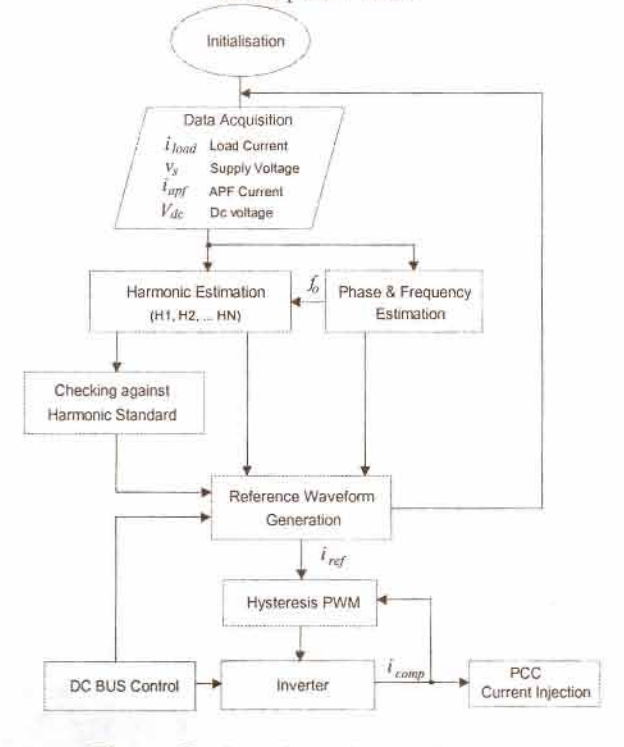


Figure 2 Flow chart of Control Strategy.

The estimated harmonic waveform quantities

together with the level of compensation are used to generate the reference waveform for the PWM pattern generator. The PWM switching module controls the inverter output in order to track the reference waveform. The inverter injects the synthesised reference current into the mains supply ac at the point of common coupling.

2-2- Harmonic Estimation

Non-linear loads in power systems are often dynamic in nature such that the distortion level and the magnitude of the load current vary continuously with time and load conditions [12]. This section proposes an adaptive algorithm to track and estimate the time varying magnitudes and phases of the load current harmonics.

The proposed harmonic estimation process is illustrated in Figure 3. It consists of a phase and frequency tracking technique and a parallel filter bank that performs the harmonic estimation. The fundamental frequency of the power system voltage, f_o , and phase, ϕ_o , are tracked by a phase and frequency estimator. The estimated frequency is then used by a resonator based parallel filter bank (RBFB) to determine the individual harmonic components of the load current, i(n). The phase and magnitude of each harmonic, filtered out by filter bank, can be calculated using a sliding measurement algorithm [13]. The calculated magnitude of each harmonic is used to find the active power filter reference waveform, iref, for harmonic reduction and/or reactive power compensation.

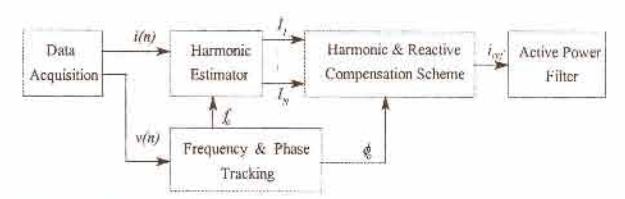


Figure 3 Proposed harmonic estimation technique for active power filtering.

2-2-1- Resonator Filter Bank

The structure of the proposed filter bank based harmonic estimation scheme is shown in Figure 4. The filter bank consists of parallel digital resonators with a common feedback loop referred to as a resonator based filter bank [14-16]. The

transfer function from the input signal, x(n), to the residual error signal, e(n), is equivalent to an IIR band pass filter whose zero transmission frequencies are at ω_k for k=1, ..., N. Also, the transfer function from the input to the output of each filter is exactly unity at the resonant frequency of the corresponding resonator and zero at the frequencies of all the other resonators [15, 16]. For the proposed filter bank structure illustrated in Figure 4, the transfer function of each resonator is given by [15]:

$$H_r^k(z) = \frac{a_k z^{-1} - z^{-2}}{1 - 2a_k z^{-1} + z^{-2}}$$
 (1)

where $a_k = cos(\omega_k)$ and ω_k is equal to the k^{th} harmonic angular frequency. The transfer function from the input, x(n), to the output of each resonator, $y_k(n)$, is equivalent to an IIR band-pass filter as follows:

$$H_{BP}^{k}(z) = 2g \frac{a_k z^{-1} - z^{-2}}{1 - 2a_k z^{-1} + z^{-2}} H_n(z)$$
 (2)

$$H_{BP}^{k}(z) = 2g \frac{a_{k}z^{-1} - z^{-2}}{1 - 2a_{n}z^{-1} + z^{-2}} H_{n}(z)$$
 (3)

where

$$H_{BP}^{k}(z) = 2g \frac{a_k z^{-1} - z^{-2}}{1 - 2a_k z^{-1} + z^{-2}} H_n(z)$$
 (4)

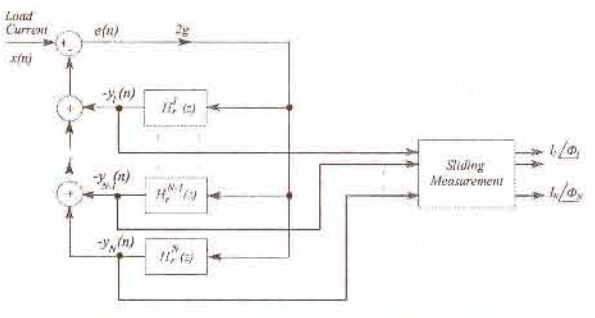


Figure 4 Resonator based filter bank.

The resonator frequency of each filter should be adapted to match the frequencies of the input data. When the filter has converged, the isolated input sinusoids are available at the outputs of the resonators. Figure 5 shows the magnitude response of the filter bank for N=4 and frequencies of 32, 100, 150, 200 Hz. As seen in Figure 5, the zero transmission frequencies of each filter in filter bank are located at the bandpass frequencies of

other filters. The frequency of 32 Hz is chosen in order to show the filtering capability of the filter bank for sub-harmonic or non-integer harmonic components.

The residual error signal, e(n), of the filter bank structure (Figure 4) can be monitored to identify transient periods caused by frequency and/or magnitude changes in load current. In steady state conditions this error converges to a minimum value while during transient periods it reaches a maximum value.

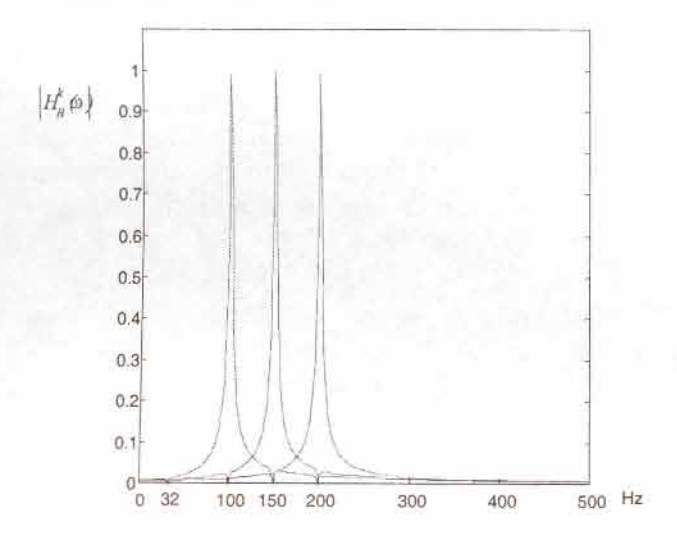


Figure 5 The magnitude transfer functions the filter bank for N = 4 and g = 0.01: $f_1 = 32$ Hz, $f_2 = 100$ Hz, $f_3 = 150$ Hz, $f_4 = 200$ Hz [15].

2-3- Frequency Tracking

Online estimation of the load current harmonics in time-varying conditions requires accurate frequency and phase estimation of fundamental component. The fundamental frequency is used to adjust the centre frequency of each filter in the filter bank [17]. A digital FM demodulator is proposed to track the variation of the fundamental power system frequency (signal in FM) from 50 Hz (carrier in FM) [18]. Figure 6 shows the block diagram of the proposed FM demodulation technique used for fundamental frequency tracking.

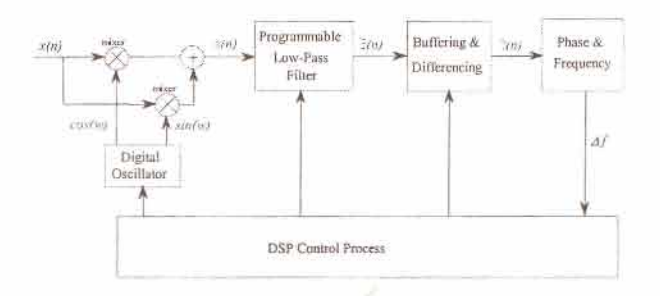


Figure 6 Digital FM demodulator frequency tracking.

3- Harmonic Reduction Schemes

The existing control methodologies for active power filter are distinguished by how the current reference signal for the harmonic reduction is derived from the measured quantities. In proposed control methodology several harmonic reduction can he employed which way the harmonic differentiated the by components are included in reference current waveform. These include full compensation, selective and harmonic standard based reduction schemes.

3-1- Full Compensation Scheme

In full compensation scheme the active power filter reference waveform, $i_{ref}(t)$ includes all retrieved harmonics from the harmonic estimation module. It can also include the reactive power for power factor correction if necessary. The reference waveform for full compensation scheme can be calculated as:

$$i_{ref}(t) = K_{reactive} * i_{reactive}(t) + \sum_{h=2}^{N} i_h(t)$$
 (5)

where $K_{reactive}$ is a constant which controls the level of fundamental reactive power compensation.

3-2- Selective Harmonic reduction Scheme

In a selective harmonic reduction scheme, the most important and dominant low order harmonics can be chosen to be compensated. In this scheme the APF reference waveform is determined as follows:

$$i_{ref}(t) = K_{reactive} * i_{reactive}(t) +$$

$$\sum_{h=j}^{N} i_h(t) \ (j = j_1, j_2, j_3, j_4, \cdots)$$
(6)

where $j_1, j_2, ..., j_M$ are the order of the selected harmonic components for reduction.

3-3- Standard Based Harmonic Reduction Scheme

In order to meet the harmonic standard requirements the magnitude of each estimated harmonic waveform is compared against the recommended values by harmonic standard. If they exceed the recommended values they will be reduced to the desired level such that harmonic standard recommendations are not exceeded. The active power filter reference waveform is calculated as follows:

$$i_{ref}(t) = K_{reactive} * i_{reactive}(t) + \sum_{h=2}^{N} I_h^{ref} * i_h(t)$$
 (7)

where I_h^{ref} is the reference load current weighting factor for each harmonic component. The objective of partial compensation in this scheme is to reduce the magnitude of the individual harmonic components, I_h , to K% of the fundamental magnitude, I_l .

$$i_{h}^{new}(t) \leq K i_{1}(t) , i_{h}^{apf}(t) = i_{h}(t) - i_{h}^{new}(t)$$
and
$$i_{h}^{apf}(t) = I_{h}^{ref} * i_{h}(t) , I_{h}^{ref} = (1 - \frac{K*I_{1}}{I_{h}})$$
(8)

where i_h^{new} and i_h^{apf} are the h^{th} load harmonic component after compensation and h^{th} component of the reference compensating current (active power filter current). Finally the I_h^{ref} is determined as follows:

if
$$(I_h > K_1 K_h^{std} * I_1)$$
 then
$$I_h^{ref} = (1 - \frac{K_1 K_h^{std} * I_1}{I_h}), else \quad I_h^{ref} = 0.0$$
(9)

where K_h^{std} is the recommended value for h^{th} harmonic component which is allowed in the supply system and K_I is the modifying factor which can be applied by end-users or utilities. I_h is the estimated magnitude for h^{th} harmonic order.

Depending to the adopted harmonic standard the value of K_h^{sul} for current can be obtained directly from standard or can be calculated from by standard recommended limits for voltage harmonic distortion [4].

4- Simulation Results

Simulations using MATLAB [19] package have been developed to verify the proposed frequency estimation and filter bank harmonic measurement techniques.

4-1- FM Demodulation

Active power filters are largely employed for steady state conditions however, for time-varying situation the adaptation process should be able to track any changes of frequency and magnitude of the supply voltage and load current.

Figures 7 and 8 show the performance of the FM demodulation technique for a step and sinusoidal changes in frequency of the test signal. Figure shows the performance of the FM demodulation technique for two test signals with different signal to noise ratios (SNRs). Figures 7 and 8 shows the frequency tracking results using a N_{FIR} =50th order FIR filter and a SNR=25 dB. A higher order FIR (ideal low pass filter) is required when SNR is low which increases the computational burden and delay of tracking.

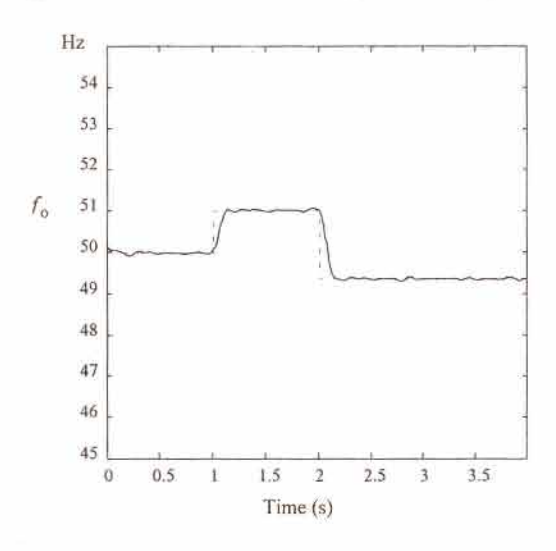


Figure 7 Fundamental frequency tracking for step changes: f_{cut} =5 Hz, N_{FIR} =50, SNR=25 dB, SNR=25 dB

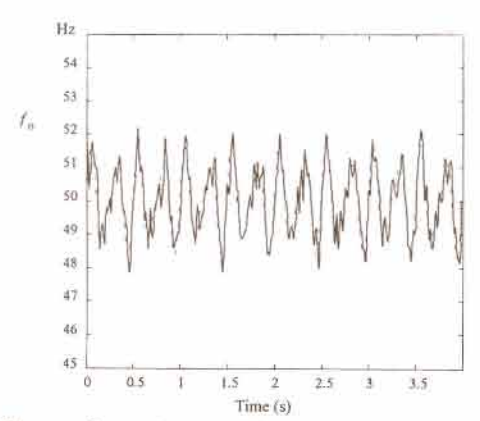


Figure 8 Fundamental frequency tracking for sinusoidal changes: $f_{cut} = 5$ Hz, $N_{FIR} = 50$, SNR=25 dB.

4-2- Filter Bank harmonic estimation

The initial band-pass frequencies of the filter bank are set to the integer multiples of the fundamental frequency. The load current and supply voltage are sampled at a frequency of 3200 Hz. Figure 9 shows the performance of the filter bank used for estimation of the fundamental frequency for a time-varying situation where both found frequency and magnitude are subjected to changes. The results indicate that this technique can track the variation in frequency and magnitude of the signal quite well. In steady state conditions the waveforms in filter bank outputs are undistorted versions of the input harmonic components and there is no phase error propagation as in the case of the cascaded line enhancer [20].

The magnitude and phase of each harmonic waveform can be calculated by the using the sliding algorithm [21]. Figure 10 shows the estimated magnitude of fundamental. As illustrated in this figure, the amplitude of the fundamental are retraced after each disturbance caused by a change in the signal frequency and magnitude.

The simulation results show that the sliding algorithm for harmonic magnitude calculations is capable of tracking changes in the input signal magnitude and frequency. The harmonic magnitude is estimated accurately when the transient in the output of the filters has decayed. As mentioned before, the transient period can be detected using the residual error signal, e(n) in

filter bank structure. It increases the stability and reliability of the process of harmonic reduction during the transient period.

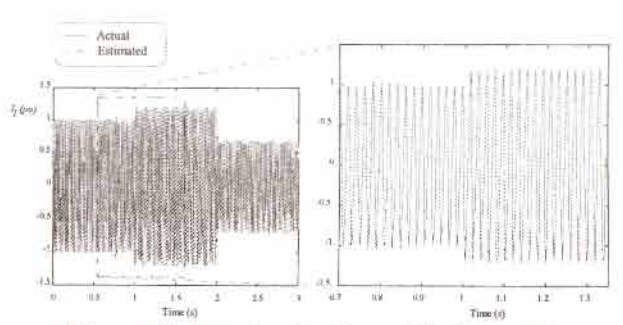


Figure 9 Actual and estimated fundamental waveforms.

5- Experimental Results

A shunt active power filter circuit has been set up to evaluate the proposed active power filter (APF) control strategy. A single-phase inverter with IGBT switches rated at 600 V (DC) and 50 A is used in these experiments.

5-1- Frequency Estimation

Figure 11 shows the performance of the FM demodulation module in tracking the signal frequency for a step change from 50 Hz to 51.66 Hz. Although step changes in the fundamental frequency is not common in power system operation, this example shows the effectiveness of this system in frequency tracking. When the noise level and harmonic distortion in the input signal are low, the order of the FIR filter employed in this technique can be reduced which further improves the performance of the frequency tracking in terms of accuracy and tracking delay.

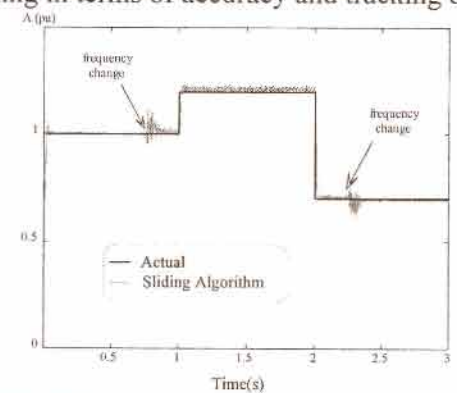


Figure 10 Actual and estimated amplitude of Fundamental.

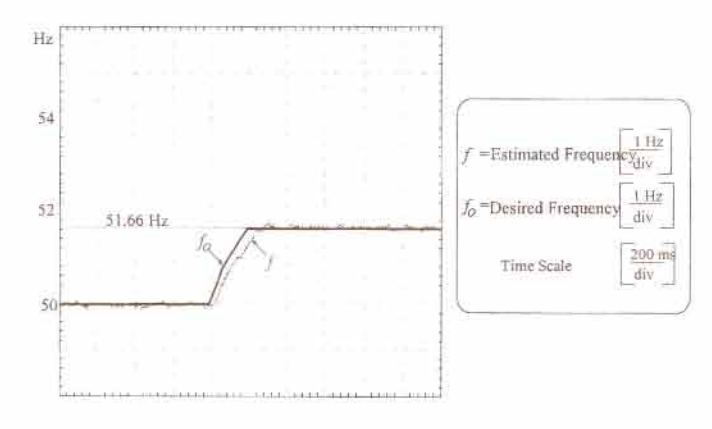


Figure 11 The estimated frequency and the voltage waveform.

5-2- Harmonic Estimation

A non-sinusoidal load current waveform has been decomposed into the fundamental and harmonic components using the filter bank module. Figures 12-14 show the estimated fundamental and harmonic waveforms of a non-linear load in steady state. The estimated waveforms at the output of the filter bank can be used to calculate the phase and magnitude of each harmonic if required. However, this is not necessary as the reconstruction of the reference waveform requires only the instantaneous magnitude of the harmonic components.

Figure 12 shows the fundamental and 3^{rd} harmonic load current waveforms. It shows the phase delay, ϕ , of the fundamental current

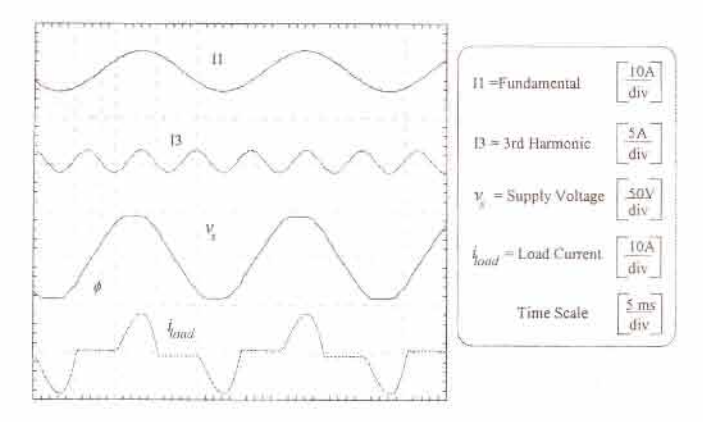


Figure 12 The estimated fundamental current (I_1) , 3^{rd} harmonic (I_3) , in relation to supply voltage (V_s) and load current (I_{load}) .

waveform with respect to the supply voltage. The phase of the supply voltage and the fundamental load current waveforms have been determined using the phase and frequency-tracking module. Figures 13-14 show the estimated harmonic current waveforms (5th -19th) for the case illustrated in Figure 12.

5-3- Harmonic Reduction Compensation

In next section the experimental results presented for full compensation and the proposed harmonic reduction schemes including selective and harmonic standard based harmonic reduction schemes.

5-3-1- Full Harmonic Compensation

In this experiment, no harmonic limits are applied in relation to harmonic compensation. The experimental results for full compensation are presented in Figure 15. It shows the load current and source current waveforms after compensation. The active power filter current, *iapp*, includes all harmonic components of the load current. As seen the injection of the active filter current into the point of common coupling using the PWM switching strategy introduces some high frequency components that can be removed by using a high pass-filter.

Figure 16(a) shows the frequency spectrum of the source current waveform before compensation. As shown in Figure 16(a), the odd harmonics are the dominant harmonic components. Figure 6(b) shows the frequency spectrum of the source current after harmonic compensation. As seen in this figure the low order harmonics have been effectively compensated. The fundamental current after compensation is slightly higher than the fundamental before compensation. This is due to the fundamental current drawn by the inverter to compensate for its switching losses. The total harmonic distortion (THD) of the source current in this experiment is calculated to be 62.8% before reduction and 5.7% after reduction, which is satisfactory for an average switching frequency of 4 kHz of the inverter.

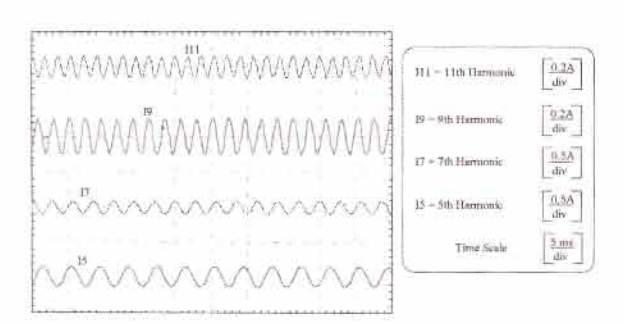


Figure 13 The estimated current harmonic waveforms: 11th, 9th, 7th and 5th.

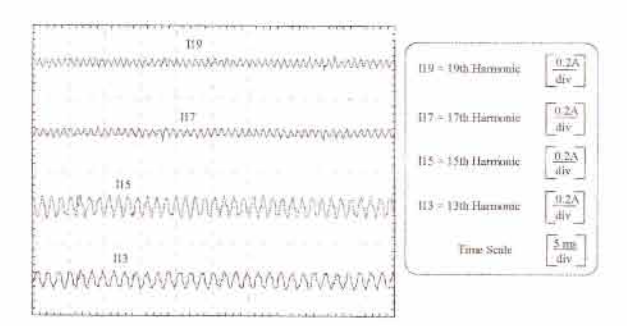


Figure 14 The estimated current harmonic waveforms: 19th, 17th, 15th and 13th.

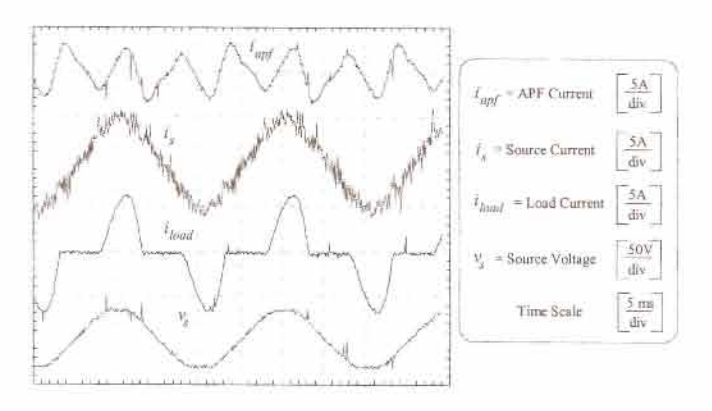


Figure 15 Full harmonic compensation scheme.

5-3-2- Selective harmonic reduction

In selective harmonic reduction one or a set of harmonic components can be compensated. Figures 17-21 show the experimental results for the three selective reduction schemes. In these schemes 3rd, 5th, 7th harmonic components are compensated separately or in a combined fashion.

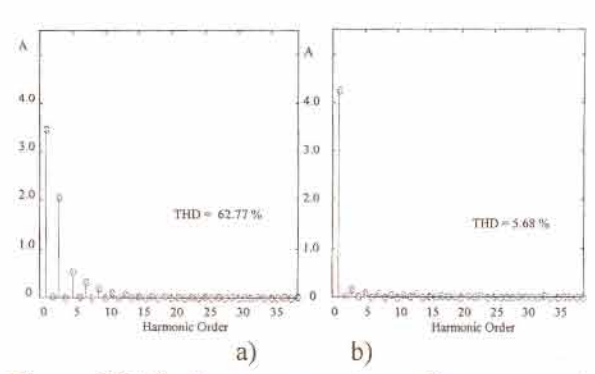


Figure 16 The frequency spectrum of source current; (a) before and (b) after compensation.

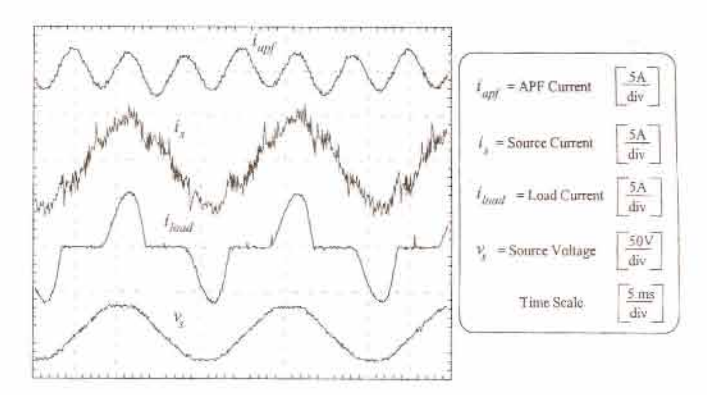


Figure 17 Selective harmonic reduction; 3rd harmonic.

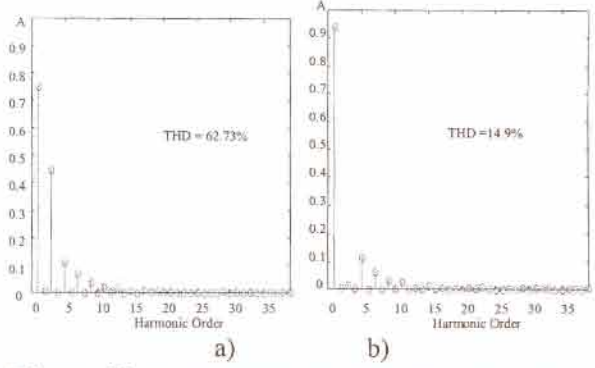


Figure 18 The frequency spectrum of source current for 3rd harmonic reduction (a) before and (b) after reduction.

5-3-3- 3rd harmonic reduction

Figure 17 shows the experimental results for 3rd harmonic cancellation. The magnitude of the 3rd harmonic current component is about half of the fundamental current. The APF reference current waveform only includes the 3rd harmonic and a small magnitude of fundamental current to

compensate for the switching losses. As the 3rd mpensate for the switching losses. As the 3rd harmonic is the largest harmonic component of the load current, the source current after reduction is close in its shape to a sinusoid.

Figure 18 shows the harmonic spectrum of the source current before and after reduction. As the 3rd harmonic is the main and largest component of the load current a significant drop in total harmonic distortion (THD) occurs after reduction (from nearly 62.8% to 14.9%).

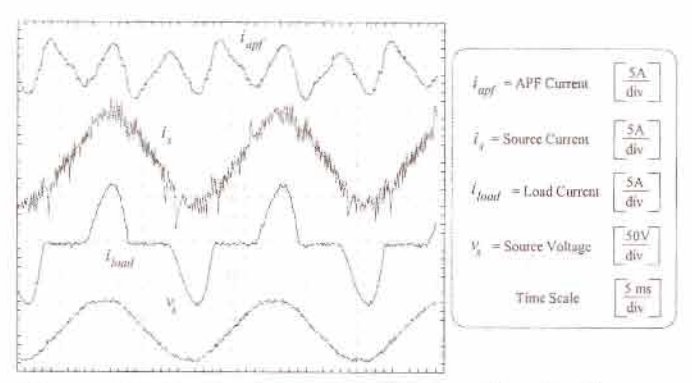


Figure 19 Selective harmonic reduction; 3rd +5th +7th harmonics.

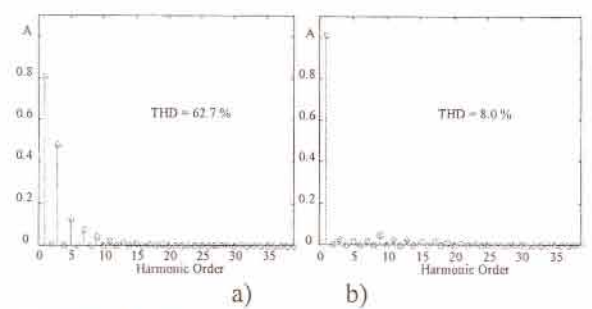


Figure 20 The frequency spectrum of source current for $3^{rd} + 5^{th} + 7^{th}$ harmonic reduction (a) before and (b) after reduction.

5-3-4- $3^{rd} + 5^{th} + 7^{th}$ harmonic reduction

The experimental results for combined reduction of 3rd, 5th and 7th harmonic components are presented in Figures 19 and 20 without and with reactive compensations respectively. The corresponding frequency spectra of the source and load current waveforms are shown in Figures 20 and 1.

Figure 19 shows the harmonic reduction without any power factor correction. The source

current still shows the phase delay with respect to the supply voltage. Figure 20 shows the frequency spectrum of the source current before and after reduction. The THD level has been reduced from 62.7% to 8.0% that is very close the fullcompensation scheme (Figure 16).

Figure 21 shows the experimental results for the same scheme but with fundamental reactive power compensation. The phase difference of the source current waveform with respect to the supply voltage has been reduced from 27° in Figure 19 to 9° in Figure 21 (ie. $cos(\phi)$ from 89% to 98%). The THD of the source current is decreased from 62.1% to 10.2% as shown in Figure 22 The reason for an increase in THD in the second case (harmonic reduction and reactive power compensation) is the reduction of the source fundamental current obtained by power factor correction.

5-4- Standards Based Harmonic Reduction

For the proposed harmonic reduction scheme based on harmonic standards, the individual harmonic voltage ratio, K_h^{std} , and the total harmonic distortion of voltage (THDV) due to non-linear load current at the point of common coupling (PCC) should be kept below the levels recommended by harmonic standards.

The value for K_h^{sul} is determined based on several parameters including the load power, supply system impedances and short circuit current at PCC. In order to verify the proposed concept for partial harmonic standard based reduction, K_h^{std} has been chosen to be a constant for all harmonic orders. Three values of $K_1 K_h^{std} = 5\%$, 10% and 15% are chosen. Figures 23 and 24 show the experimental results for APF, load and source current waveforms and frequency spectrums respectively. In this scheme all source current harmonic magnitudes should be kept below 5% of the fundamental current. As shown in Figure 24-a, the 3rd, 5th and 7th harmonic components exceed 5% of the fundamental. Therefore, the APF current contains the 3rd, 5th and 7th harmonics. The total harmonic distortion in the source current is reduced from nearly 51.3% to 11.9% in Figure 24-b. The performance of the APF in this scheme is similar to the

selective 3rd harmonic reduction scheme.

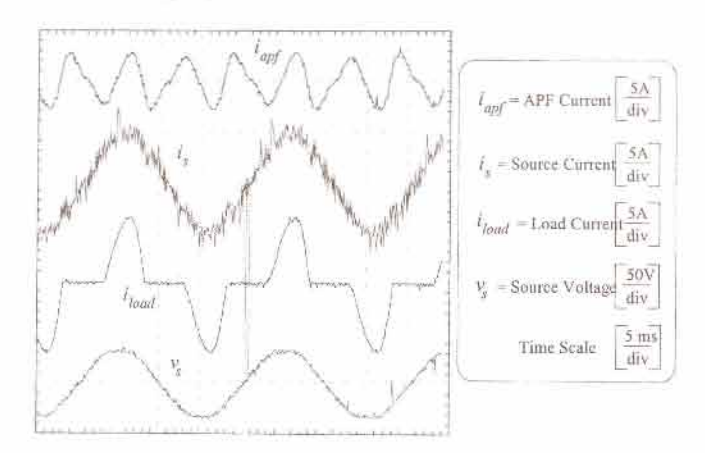


Figure 21 Selective harmonic reduction; 3rd +5th +7th harmonics and reactive power reduction.

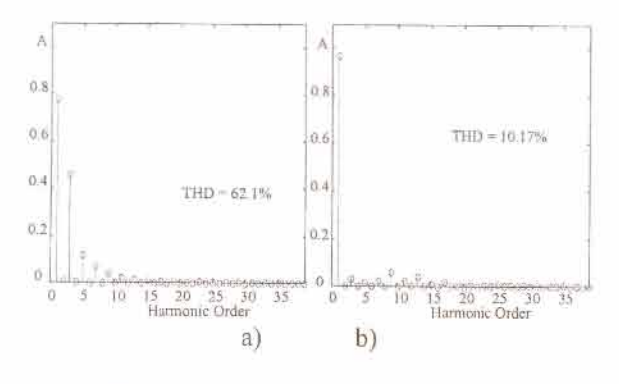


Figure 22: The frequency spectrum of source current for 3rd +5th +7th harmonic reduction (a) before and (b) after reduction with reactive power.

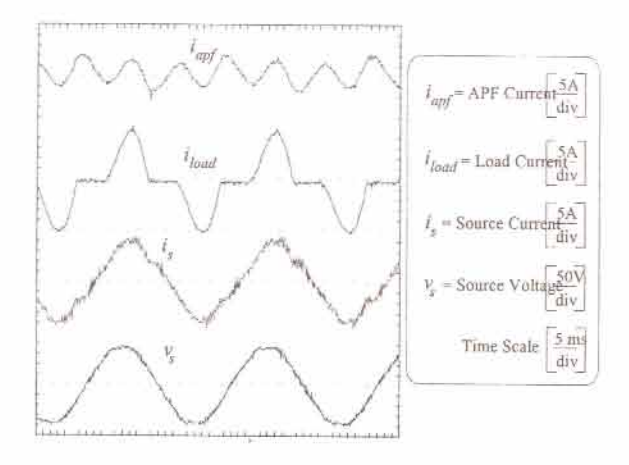


Figure 23: The 5% harmonic reduction scheme.

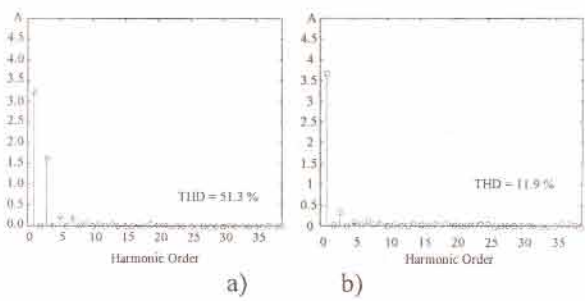


Figure 24: The frequency spectrum of source current for 5% reduction scheme:

(a) before and (b) after reduction.

Table 1 shows the magnitude of the fundamental source current, i_{sl} , the maximum APF current, i_{apf} , the real power of the APF, p_{apf} , and the maximum apparent power of the APF, $p_{apf(max)}$, for all implemented schemes. As seen from Table 1, reduction of the level of harmonic reduction (increasing K_h^{sul}) reduces the power of the active power filter. For example, the maximum apparent power of the APF is reduced from 113 VA in full compensation to 103 VA when the $K_h^{sul} = 5\%$ scheme is applied; a reduction of almost 9% in the active power filter rating.

Table 1 The comparison of the selected schemes for harmonic reduction.

Standa rd levels K_h^{stil}	(A)	i _{apf(m} ax) (A)	Pupf (W)	Papf(max) (VA)	befor e comp	THD after comp.
Full (0%)	2.6	2.6	3.8	113	51	4
5%	2.6	1.8	2.7	103	51	12
10%	2.6	1.6	1.9	105	51	15
15%	2.6	1.3	1.6	98	50	22
20%	2.5	1.2	1.1	72	51	26

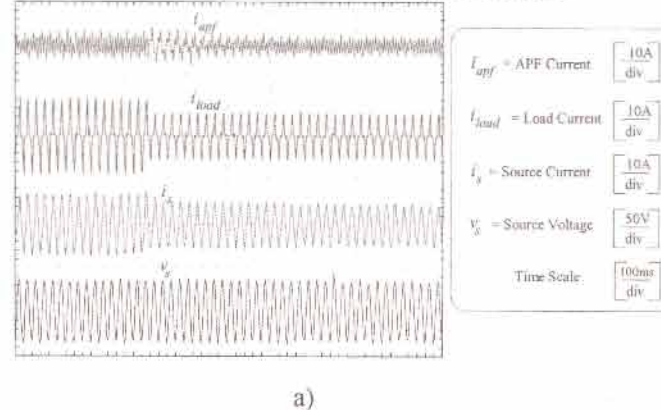
5-5- Transient Performance

The transient performance of the active power filter is tested for a step change in the load current magnitude up to twice the steady state load current. This sudden change from full load to half load working conditions and vice versa is illustrated in Figure 25. As shown in Figure 25, line current reaches steady state in almost three cycles after the step change had occurred. The delay associated with the time response of the system is due to the filter settling time in the harmonic estimation module.

6- Conclusions

A new adaptive control strategy for shunt active power filter has been proposed. The proposed control strategy for active power filtering is verified through simulation and experimental results on a laboratory prototype active power filter.

The experimental results in relation to the performance evaluation of the FM demodulation based frequency tracking technique are illustrated. The time-varying frequency of the input signal is identified for slow varying and transient conditions. The estimated fundamental frequency is used to adjust the parameters of the filter bank for harmonic retrieval of a non-sinusoidal load current waveform in time varying condition. It has been shown that the proposed control strategy is capable of accurate estimation of individual harmonic waveforms in time-varying conditions.



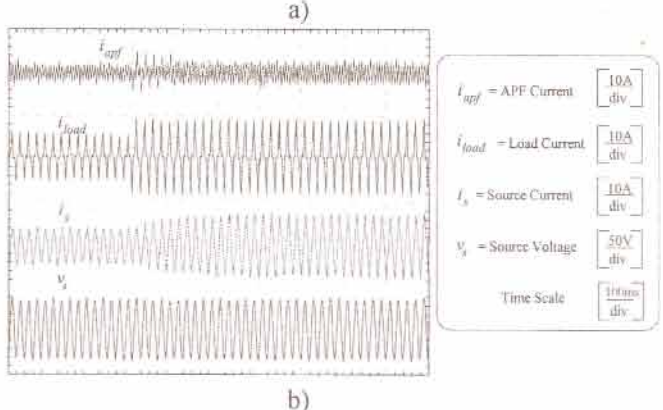


Figure 25: Transient Performance of APF with harmonic standard (5%); a) decreasing load and b) increasing load

The capabilities of the proposed harmonic estimation and measurement techniques have been employed for selective and partial harmonic reduction in active power filtering. The

experimental results have been presented for proposed selective and partial harmonic reduction schemes including the cancellation of the 3rd, 5th, 7th and their combinations with and without reactive power compensation. It is found that the proposed control strategy for harmonic compensation gives flexibility in terms of selective and partial harmonic and reactive power compensations. Experimental results show that by employing selective and partial harmonic schemes a significant reduction in active power filter rating can be achieved while the load harmonic current components can be reduced up to recommended values set by standards.

7- References

- [1] R. G. Ellis, "Harmonic analysis of industrial power systems," IEEE Transactions on Industry Applications, vol. 32, pp. 417-421, 1996.
- [2] IEC-555-2, "Disturbances in Supply Systems Caused by Household Applications and Similar Electrical Equipment, part2: Harmonics," International Electrotechnical Commission, Geneva 1982.
- [3] IEEE Std 519, "IEEE Recommended Practice and Requirement for Harmonic Control in Electric Power Systems," The Institute of Electrical and Electronics Engineers, IEEE, New York, Standard 1993.
- [4] AS-2279.2, "Disturbances in mains supply networks Part 2: Limitation of harmonics caused by industrial equipment," Australian Standards, Standard AS2279, 1991.
- [5] AS/NZS-61000.3.2, "Electromagnetic compatibility (EMC) Part 3.2: Limits—Limits for harmonic current emissions (equipment input current less than or equal to 16 A per phase)," Australian Standard, Standard AS/NZS 61000.3.3, 1998.
- [6] L. Gyugyi, "Active AC Power Filters," presented at IEEE-IAS Annual Meeting, 1976.
- [7] Keiji Wada, Hideaki Fujita, Hirofumi Akagi: "Considerations of a Shunt Active Filter Based on Voltage Detection for Installation on a Long Distribution Feeder," *IEEE/IAS Annual Meeting*, pp. 157-163, 2001
- [8] H. Akagi, Y. Kanazawa, and A. Nabae, "Instantaneous Reactive Power Compensators

- comprising Switching Device without Energy Storage Components," *IEEE Transactions on Industry Applications*, vol. IA-20, pp. 625-630, 1984.
- [9] 1. S. Srianthumrong, H. Fujita, H. Akagi, "Stability analysis of a series active filter integrated with a double-series diode rectifier," *IEEE Transaction on Power Electronics*, vol. 17, no. 1, Jan., pp. 117-124, 2002.
- [10] H. Akagi, "New trends in active filters for power conditioning," *IEEE Transactions on Industry Applications*, vol. 32, pp. 1312-1322, 1996.
- [11] S. Bhattacharya, D. M. Divan, and B. Banerjee, "Active filter solutions for utility interface," *IEEE International Symposium on Industrial Electronics*, vol. 1, pp. 53-63, 1995.
- [12] C. S. Moo, Y. N. Chang, and P. P. Mok, "A Digital measurement scheme for time-varying transient harmonics," *IEEE Transactions on Power Delivery*, vol. 10, pp. 588-594, 1995.
- [13] M. T. Kilani and J. F. Chicharo, "Relationship between the LMS and Goertzel algorithms for Fourier coefficients estimation at arbitrary frequencies," *IEEE Transactions* on Circuits and Systems, 1996.
- [14] G. Peceli, "Resonator-based digital filters," IEEE Transactions on Circuits Systems, vol. CAS-36, pp. 156-159, 1989.
- [15] M. T. Kilani, "Multifrequency signal enhancement and estimation using IIR filter bank structures," 1995, PhD Thesis, University of Wollongong, Wollongong Australia, pp. 163.

- [16] M. Padmanabhan and K. Martin, "Resonator-based filter-banks for frequency-domain applications," *IEEE Transactions on Circuits and Systems*, vol. 38, pp. 1145-1159, 1991.
- [17] A. Yazdian-Varjani, B. S. P. Perera, J. F. Chicharo, and M. T. Kilani, "Sliding Measurement of Power System Harmonics," presented at Australasian Universities Power Engineering Conference, AUPEC'96, Melbourne, 1996.
- [18] M. M. Begovic, P. M. Djuric, S. Dunlap, and A. G. Phadke, "Frequency tracking in power networks in the presence of harmonics," *IEEE Transactions on Power Delivery*, vol. 8, 1993.
- [19] Matlab, "Matlab: High Performance Numeric Computation and Visualization Software User's Guide,", 4.0 ed. Natic, MA: MathWorks, Inc., 1993.
- [20] A. A. Girgis, W. B. Chang, and E. B. Makram, "A digital recursive measurement scheme for on-line tracking of power system harmonics," IEEE Transactions on Power Delivery, vol. 6, pp. 1153-1160, 1991.
- [21] A. Yazdian-Varjani, "Harmonic Control Techniques for Inverters and Adaptive Active Power Filters" 1998, PhD Thesis, University of Wollongong, Wollongong Australia, pp. 140.